Available online at www.sciencedirect.com
ScienceDirect
Journal of Sound and Vibration 298 (2006) 672–687
JOURNAL OF SOUND AND VIBRATION
www.elsevier.com/locate/jsvi

Numerical assessment of fore-and-aft suspension performance to reduce whole-body vibration of wheel loader drivers

Gérard Fleury*, Pierre Mistrot

Laboratoire de Modélisation des Systèmes Mécaniques de Prévention, Institut National de Recherche et de Sécurité (INRS), Avenue de Bourgogne, F-54501 Vandoeuvre cedex, France

Accepted 8 June 2006
The peer review of this article was organised by the Guest Editor

Abstract

While driving off-road vehicles, operators are exposed to whole-body vibration acting in the fore-and-aft direction. Seat manufacturers supply products equipped with fore-and-aft suspension but only a few studies report on their performance. This work proposes a computational approach to design fore-and-aft suspensions for wheel loader seats. Field tests were conducted in a quarry to analyse the nature of vibration to which the driver was exposed. Typical input signals were recorded to be reproduced in the laboratory. Technical specifications are defined for the suspension. In order to evaluate the suspension vibration attenuation performance, a model of a sitting human body was developed and coupled to a seat model. The seat model combines the models of each suspension component. A linear two-degree-of-freedom model is used to describe the dynamic behaviour of the sitting driver. Model parameters are identified by fitting the computed apparent mass frequency response functions to the measured values. Model extensions are proposed to investigate postural effects involving variations in hands and feet positions and interaction of the driver's back with the backrest. Suspension design parameters are firstly optimized by computing the seat/man model response to sinusoidal acceleration. Four criteria including transmissibility, interaction force between the driver's back and the backrest and relative maximal displacement of the suspension are computed. A new suspension design with optimized features is proposed. Its performance is checked from calculations of the response of the seat/man model subjected to acceleration measured on the wheel loader during real work conditions. On the basis of the computed values of the SEAT factors, it is found possible to design a suspension that would increase the attenuation provided by the seat by a factor of two.

1. Introduction

Construction vehicle drivers are exposed to whole-body vibration, with levels that may exceed the action value of $0.5\,m/s^2$ set by the European Vibration Directive 2002/44/CE. According to the ISO 2631 standard [1], vertical, lateral and fore-and-aft accelerations are measured by a seat accelerometer placed between the seat pan and the driver's buttocks. To compute the daily vibration exposure, accelerations in the three directions are weighted and multiplied by a suitable factor. This factor is unity for vertical vibration but is

*Corresponding author.
E-mail address: fleury@inrs.fr (G. Fleury).

0022-460X/$ - see front matter © 2006 Published by Elsevier Ltd.
doi:10.1016/j.jsv.2006.06.034

equal to 1.4 for fore-and-aft vibration. The fore-and-aft vibration contribution to the daily exposure is therefore amplified and tends to produce vibration exposure beyond the limit value for some construction vehicles, such as wheel loaders [2]. The reduction of fore-and-aft vibration for wheel loader drivers may be achieved in several ways. As is the case for vertical vibration, track maintenance in quarries can contribute to the reduction of whole-body vibration in the fore-and-aft direction. Introduction of more efficient technical solutions by manufacturers also contributes to reduce driver's exposure to vibration [3]. Vibration attenuation may be achieved at different stages. The first stage concerns the vehicle. Some wheel loaders are equipped with ride control systems which reduce the vehicle pitching motion, and thereby reduce the fore-and-aft vibration exposure, although no study has been made to quantify their efficiency. The second stage at which attenuation occurs is at the seat level. Although fore-and-aft suspended seats are available on the market, most of the wheel loaders are equipped with seats without suspension in the fore-and-aft direction. Integration of a suspension in the fore-and-aft direction is considered as a good option to reduce vibration exposure in that direction. The overall aim of this work is to assess the performance of a fore-and-aft suspended seat for applications in wheel loaders.

As a first step, field measurements are conducted in real work conditions with a wheel loader in order to analyse the nature of mechanical loads applied to the operator and to characterize the postures which are adopted while driving. A numerical approach is investigated to design fore-and-aft suspensions with higher performance. This approach requires the development of a seat/man model. Laboratory tests were carried out to measure the dynamic response of a seated man exposed to fore-and-aft vibration. A model for the sitting person was developed and fitted to the measured apparent mass frequency response. Model extensions are proposed to include variations in posture, including those observed during real work conditions. Performance criteria are selected and computed for the seat/man model exposed to sinusoidal accelerations. A sensitivity analysis is performed to define optimized suspension design characteristics. As a second step, the seat/man model response with the optimized suspension is computed with the acceleration measured on the wheel loader in real work conditions. The results are post-processed according to the ISO-2631 standard and SEAT factor is computed and compared with that provided by the original seat.

2. Field testing

2.1. Field measurements in a gravel pit

2.1.1. Test conditions

The wheel loader used for field testing has an operating weight of about 11 tons and can be used with buckets of capacity between 1.6 and 5.0 m^3. The vehicle is equipped with an industrial seat, suspended in both vertical and fore-and-aft directions. The vertical suspension consists of a gas spring and a hydraulic damper and the fore-and-aft suspension consists of two pre-constrained steel springs and a hydraulic damper. The horizontal suspension stroke is symmetric.

Accelerometers were fixed at several locations in the cab to measure the fore-and-aft acceleration of the mobile part of the suspension and both fore-and-aft and vertical accelerations at the vehicle floor. Three cameras were used to film the driver's posture and motion by focusing on the driver's feet, hands and contact area between the back and the backrest. A fourth camera, mounted inside the cab, was used to film the relative displacement of the fore-and-aft suspension. The data acquisition system used permits the post-synchronization of all videos with respect to analogue measures and therefore detailed analysis was made possible to search events likely to explain a measured feature.

The main objective of performing field measurements was to characterize the nature of fore-and-aft vibration and their impact on the operator while driving during normal operations. Measurements were performed on the wheel loader during loading and carrying operations in a gravel pit. The wheel loader operator was asked to feed a crusher with gravel stocked in a heap. A work cycle carried out by an experienced worker lasted about one and a half-minute. In total, 30 s were required to carry materials on quarry tracks: 10 s were needed to empty the bucket and 20 s to load it. A first set of cycles were recorded with the fore-and-aft suspension in the locked position, while it was unlocked in a second phase. The entire recording lasts about 15 min.

2.1.2. Results

The sitting driver leans against the backrest over the entire back surface and holds the steering wheel either with both hands during carrying operation or only with one hand when handling, while the other hand is placed on the levers to control the hydraulic function for fork and bucket. His arms are never stretched. The driver's feet are in contact with the pedals to brake or to accelerate but most of his weight is obviously supported by the seat pan.

The fore-and-aft acceleration spectrum measured on the vehicle floor shows that the vibration energy is higher in two frequency ranges. The first range is characterized by frequencies lower than 0.01 Hz. These include the working cycle frequency. Therefore it is assumed that events, like bucket loading, occurring once per working cycle and generating high fore-and-aft acceleration provide high energy content. The second frequency range occurs between 1.5 and 2.0 Hz and includes the vehicle eigenfrequency associated with the pitching motion occurring while riding over a rough terrain with potholes.

At the end of the tests, the driver was asked to assess the comfort associated with the use of a fore-and-aft suspension. In general, more comfort was felt when the suspension was unlocked. Analysis of the videos focusing on the fore-and-aft suspension allows to quantify approximately how long the suspension is activated by selecting all the sequences during which a relative suspension displacement is detected. Results show that the fore-and-aft suspension works during almost 20% of the time, as opposed to 90% for the vertical suspension. Highest relative displacements were observed during operations involving bucket loading. This operation is very short but produces shocks with high acceleration levels. Significant relative displacements of the fore-and-aft suspension were also observed during riding operations to transport materials. For this type of operation, the displacement is not as high as during bucket loading but the exposure duration is longer. Consequently, it is considered important to assess fore-and-aft seat performance for wheel loaders by taking into account shocks due to bucket loading and fore-and-aft vibration resulting from the vehicle pitching motion observed while transporting. This was done by considering each of these conditions separately by performing representative operations. Measurements consisted in recording the acceleration on the wheel loader to obtain representative signals to be reproduced in the laboratory to assess the seat performance under each of these two conditions.

2.2. Ridding tests on a normalized wood track

2.2.1. Test conditions

The wheel loader is equipped with a ride control system, which consists in gas/oil accumulators connected to the lift cylinder of the fork to absorb shocks and smooth out the ride to increase operator comfort. In order to exclude the influence of such a system, the ride control system was disabled during the carrying tests. To increase repeatability, carrying tests were performed on a normalized NIAE wood track designed according to ISO 5008 standard [4] and usually used for testing agricultural machines. The track length was 100 m and tests were performed at vehicle speeds of 7, 9, 12, 15 and 18 km/h, which were controlled by reading the tachometer. These tests were conducted with an empty bucket (Figs. 1–4).

2.2.2. Results and analysis

Table 1 reports fore-and-aft unweighted rms acceleration values recorded on the vehicle floor. An increase of the vehicle velocity up to 10 km/h leads to an increase of the fore-and-aft rms acceleration values. The video

Fig. 1. Wheel loader and its suspended seat.

Fig. 2. Instrumentation of the cab with accelerometers and cameras.

Fig. 3. The four views recorded in the cab: (a) hand location; (b) contact area back/backrest; (c) fore-and-aft suspension; (d) foot position.

analysis of the global motion of the wheel loader shows that the pitching motion becomes more important with increased velocity. Therefore, fore-and-aft accelerations are assumed to result from the pitching motion of the vehicle. Fore-and-aft rms acceleration values reach a maximum at a velocity of 10 km/h. For this reason, the acceleration recorded at that speed is considered for further analysis.

The spectral analysis of the signal in Fig. 5 shows that the frequency of peak vibration energy occurs at approximately 1.6 Hz, which is in agreement with the acceleration signal measured during work conditions in the gravel pit. This signal is thus selected to be reproduced in the laboratory to assess the seat performance for carrying operations of a wheel loader.

2.3. *Bucket loading tests at a heap*

2.3.1. *Test conditions*

The operator was asked to drive forward to the heap, fill the bucket, drive backward and forward and empty the bucket at the same heap. The suspension was unlocked. The driver held the steering wheel

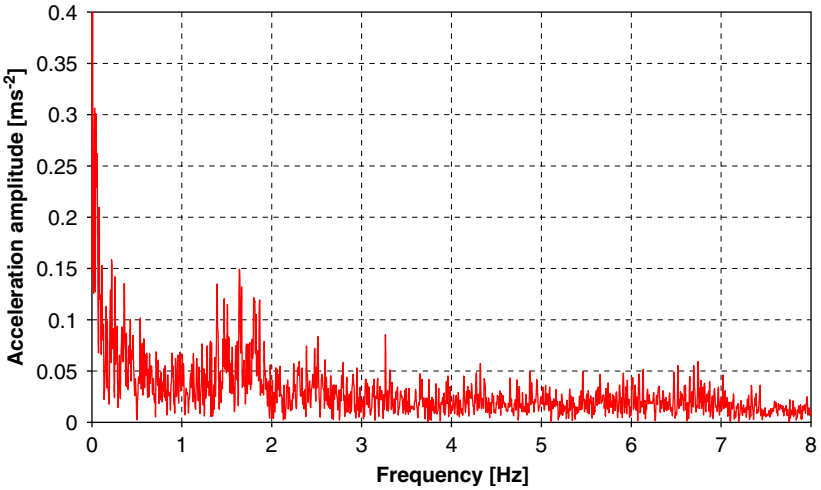

Fig. 4. Spectrum of fore-and-aft acceleration measured on the floor of a wheel loader during loading and carrying operations in a quarry.

Table 1
Fore-and-aft unweighted rms acceleration measured on the wheel loader floor while riding at several speeds on an NIAE tests track

Estimated velocity from the tachometer (km/h)	Mean velocity (km/h)	Fore-and-aft rms acceleration measured on the vehicle floor (m/s^2)
7	5	0.4
9	4	0.5
12	10	1.1
17	14	0.8
15	15	0.9

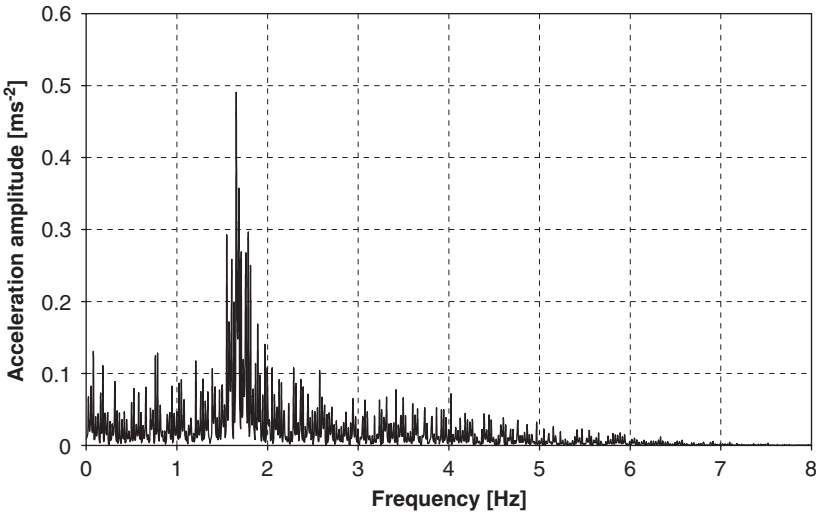

Fig. 5. Spectrum of the fore-and-aft acceleration measured on the vehicle floor during riding test over the NIAE test track at 10 km/h.

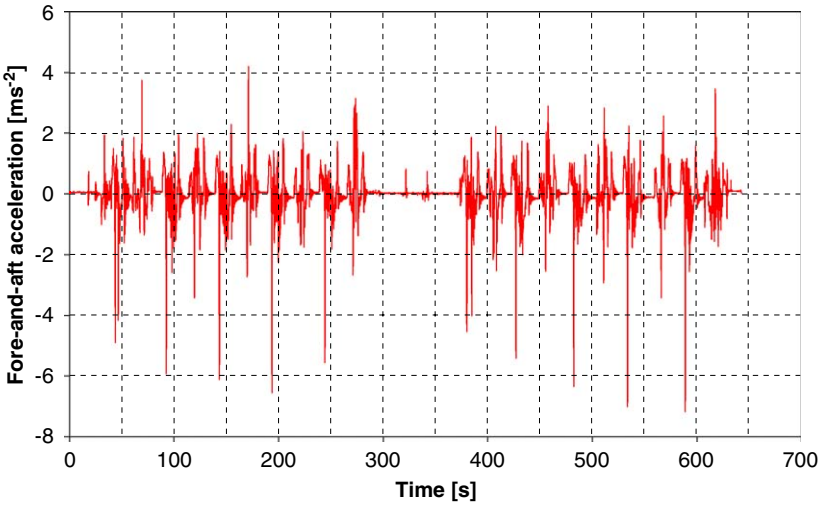

Fig. 6. Fore-and-aft acceleration time histories measured on the vehicle floor during 10 loading/unloading cycles.

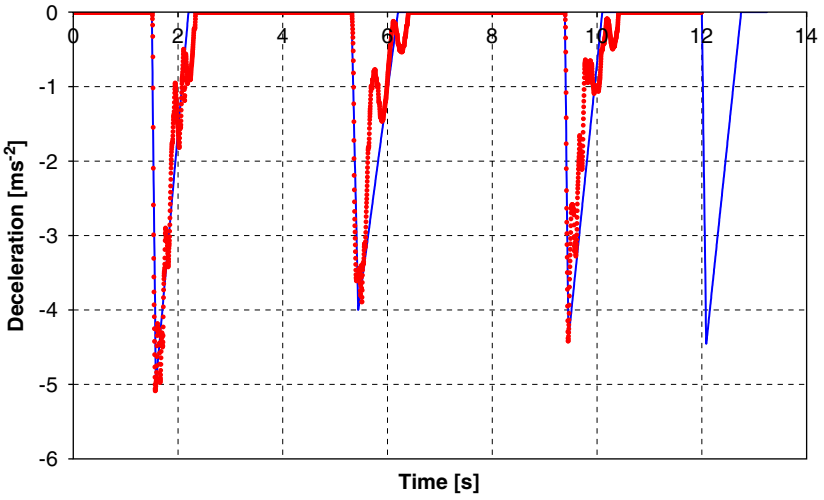

Fig. 7. Measured (dots) and idealized (lines) initial shock signals occurring during bucket loading.

with one hand and used the other one to actuate the hydraulic levers to control fork and bucket. Fig. 6 shows the fore-and-aft acceleration recorded on the vehicle floor during 10 operation cycles.

2.3.2. Results and analysis

Each cycle shows a deceleration peak of about 6 m/s^2 resulting from the bucket driving in the heap, followed by secondary peaks with lower magnitude. The maximal deceleration peak lasts at least 1 s, is negative in the fore direction and hence causes a significant relative displacement of the mobile part of the suspension with respect to the vehicle floor in the fore direction. In most cases, the suspension stroke in that direction is not high enough and bottoming occurs. The initial maximal deceleration peak is selected to build a shock signal to be reproduced in the laboratory. Fig. 7 shows three of these initial peaks measured during bucket loading. Signals are idealized as triangles. The fourth triangle shown in Fig. 7 is the average of the first three one and is selected to be representative of the shock signals to be reproduced in the laboratory to assess seat performance when loading the wheel loader.

The idealized signal has a maximal deceleration value of $4.5\,m/s^2$ reached after 0.1 s. The deceleration peak lasts 0.9 s. Double integration of this acceleration signal while setting the initial velocity equal to zero leads to an absolute displacement of 1 m.

3. Measurement of the apparent mass of a seated subject exposed to fore-and-aft random vibration

3.1. Experimental method

The assessment of fore-and-aft suspension performance using numerical tools requires the development of a model to describe the dynamic behaviour of a seated subject exposed to fore-and-aft vibration. Model parameters are identified by fitting experimental data. Thus, the apparent mass frequency response of one seated subject was measured in the fore-and-aft direction using random vibration with rms acceleration of $1.2\,m/s^2$ in the frequency range from 0.5 to 8 Hz. The test procedure used and all the results are fully reported in Ref. [5]. The industrial seat used for the tests in the laboratory was similar to that which was installed in the wheel loader during field testing. The seat was disassembled and the vertical suspension was removed. The seat cushion, the backrest and the fore-and-aft suspension were mounted to a frame bolted on a hydraulic shaker (see Fig. 8).

All tests were performed with the same male subject. His body mass was equal to 87 kg. A force sensor was fixed to the seat frame in order to measure the force transmitted by the suspension to the seated subject. Accelerations acting on the subject were measured by means of a seat accelerometer placed between the seat

Fig. 8. Seat mounted on a shaker to measure the apparent mass of a seated subject.

cushion and the driver's buttocks. Data acquisition and post-processing were performed by using the LMS software. The complex transfer function between force and acceleration was computed. Measurement of the apparent mass of the seat alone was performed. Real and imaginary parts of the seat apparent mass were subtracted from those of the seat-subject response function in order to obtain the apparent mass frequency response of the subject.

Experimental and modelling efforts have mainly been devoted to represent the driver's posture with hands on lap and feet supported by the floor. The fore-and-aft suspension could easily be locked or unlocked. The backrest could easily be reclined from vertical to horizontal positions. Therefore, particular attention was paid to include three tests with the following seat settings:

- fully reclined backrest and suspension locked,
- backrest inclined at 10° back and suspension locked,
- backrest inclined at 10° back and suspension unlocked.

3.2. Results and analysis of apparent mass measurements

3.2.1. Influence of frequency on apparent mass response

All apparent mass frequency response functions exhibit the same shape. At frequencies lower than 1 Hz, the apparent mass remains nearly constant and decreases slightly in some cases. With increasing frequency, the apparent mass tends to increase, reaches a maximum in the frequency range from 2 to 5 Hz, depending on the test conditions, and finally decreases to reach a value lower than 10 kg at 8 Hz. In order to investigate accurately the effect of frequency on the seated subject's response, additional tests with seat setting "fully reclined backrest and suspension locked" were conducted at a constant frequency with a sinusoidal rms acceleration of $1.2\,m/s^2$. The subject's motion due to vibration was filmed. At frequency of 0.7 Hz, a pitching motion of the subject's upper body around a transverse axis approximately located in the pelvis area was observed. This type of behaviour has already been reported by Fairley [6]. The rotational motion vanished with increasing frequencies. Hence, it is emphasized that the human body may be modelled with two interconnected rigid bodies. The connector is assumed to be a hinge with an axis located in the pelvis area and perpendicular to the sagittal plane. The rotational degree of freedom is assumed to have a stiffness and to be damped.

At a higher frequency around 2.25 Hz, videos showed that the most obvious motion was a purely fore-and-aft pelvis translation with respect to the seat pan. This out-of-phase motion caused a peak to occur in the apparent mass magnitude and a 90° phase angle. The frequency of 2.25 Hz corresponds to the main resonance of the seated subject exposed to fore-and-aft vibration.

3.2.2. Influence of the backrest on the apparent mass response

The apparent mass measured when the subject is leaning against the backrest are considerably higher than those measured without backrest support. Therefore, the backrest and the manner in which it is used by the operator should be considered to assess fore-and-aft suspension performance. The resonance frequency measured when the subject is leaning against the backrest is approximately 0.5 Hz higher than the resonance frequency obtained without backrest. If the subject does not use the backrest, interaction forces are only transmitted through the sitting surface. For the case involving the subject leaning against the backrest, additional forces are transmitted from the seat to the operator through the backrest. Thus, an additional stiffness is required to model the interaction between the seat and the subject. Higher experimental scatter is also observed on the peak apparent mass measured with the subject leaning against the backrest. Additional tests were repeated to reduce the experimental scatter. Efforts were particularly devoted to define and report with more precision the initial position of the subject's back with respect to the backrest. Two initial postures were distinguished: (i) the contact surface between the subject's back and the backrest is limited to the lumbar area, (ii) the contact surface between the subject's back and the backrest is extended to the whole back surface. This latter posture led to apparent mass peaks higher than those measured when the contact was limited to the lumbar area.

3.2.3. Influence of fore-and-aft suspension on the apparent mass response

The fore-and-aft suspension could easily be manually locked or unlocked. If unlocked, the fore-and-aft suspension transmits vibration at lower frequencies (<1 Hz) but attenuation occurs at frequencies higher than 1.5 Hz. The attenuation factor is approximately equal to one-third. Peak apparent mass when the suspension is unlocked occurs at a frequency which is approximately 0.5 Hz higher than that measured when the suspension is locked. The increase of the resonance frequency due to the use of the suspension results from the attenuation of the input signal by the suspension and the fact that the dynamic response of the seated human body is nonlinear. Additional tests carried out with locked suspension and random input vibration with rms acceleration of 0.44 m/s^2 (i.e. 1.2 m/s^2 multiplied by the attenuation factor of the suspension) produce the same apparent mass response as measured with the unlocked suspension when the rms acceleration is 1.2 m/s^2. A linear model of the sitting human can not reproduce this feature.

4. A model to predict the dynamic behaviour of the seated human body

4.1. Description of the model for a seated subject

The dynamic behaviour of a seated subject is firstly modelled for the case "hands on lap", "feet on the shaker" and "backrest off". This two-dimensional model connects two rigid bodies, where the lower body represents lower limbs and pelvis and the upper body includes the trunk, upper limbs and head of the seated human body. The lower body is connected to a rigid seat by means of a spring and a damper, both oriented in the fore-and-aft direction. The upper body is connected to the lower body by means of a hinge with rotational stiffness and damping. The upper rigid body is assumed to be rectangular and the position of its centre of gravity with respect to the hinge rotation point is required to define its moment of inertia. The model has two degrees of freedom: the fore-and-aft relative translation of the lower body with respect to the seat (x_1) and the rotation of the upper body about the hinge axis (θ). Seven parameters are required to define the model response: the two masses of both rigid bodies (M_1 and M_2), stiffness and damping coefficients for the connection between the lower body and the seat (K_1 and C_1), rotational stiffness and damping coefficient applied to the hinge (K_2 and C_2) and the distance between the centre of gravity of the upper body to the hinge axis (L).

The equations of motion are derived by assuming small rotations, i.e.

$$\sin(\theta) = \frac{x_1 - x_2}{L} \approx \theta,$$

$$M_1\ddot{x}_1 + K_1(x_1 - x_0) + C_1(\dot{x}_1 - \dot{x}_0) + M_2\ddot{x}_2 = 0, \tag{1}$$

$$J_G(\ddot{x}_1 - \ddot{x}_2) - M_2L^2\ddot{x}_2 + K_2(x_1 - x_2) + C_2(\dot{x}_1 - \dot{x}_2) = 0, \tag{2}$$

$$M = M_1\frac{x_1}{x_0} + M_2\frac{x_2}{x_0}, \tag{3}$$

where M_1, M_2 is the mass of the lower and upper rigid body, respectively, θ the rotational angle in the hinge, x_0, x_1, x_2 the complex fore-and-aft displacement of the excitation point, the lower rigid body and the upper rigid body, respectively, L the distance between the hinge axis and the centre of gravity of the upper rigid body, J_G the moment of inertia of the upper rigid body with respect to its centre of gravity, K_1, C_1 the stiffness and damping coefficient of the connector between the lower rigid body and the excitation point, K_2, C_2 the rotational stiffness and damping coefficient applied to the hinge.

4.2. Parameter identification by fitting apparent mass response

The masses of the lower and upper body are given by Plagenhoef in Ref. [7], where each body segment's weight is given as a percentage of total body weight. The distance between the centre of gravity of the upper body to the hinge axis is assumed to be equal to 0.4 m. The peak apparent mass and the corresponding frequency are expressed as polynomials in the stiffness K_1 and the damping coefficient C_1. K_1 and C_1 are

analytically calculated by seeking polynomial solutions satisfying the measured peak apparent mass. The stiffness K_2 is arbitrarily fixed and the damping coefficient C_2 is analytically calculated by seeking polynomial solutions satisfying the apparent mass value measured at 0.7 Hz.

4.3. Seated subject model extensions

Model extensions are proposed to include postural effects on the apparent mass. The effect of setting the feet on a footrest is modelled by adding a mass of 7 kg to the lower body. The effect of setting the hand on the steering wheel is taken into account by constraining the fore-and-aft translation at the upper extremity of the upper body.

Experimental results indicate that the use of the backrest and the manner by which the contact is established have a considerable effect on the apparent mass response function. The effect of leaning against the backrest is taken into account by adding a spring (K_3) and a damper (C_3) between the lower rigid body and the rigid seat. If the driver makes contact with the backrest only in the lumbar area, a transfer of weight from the upper to the lower rigid mass is considered. If the driver leans against the entire backrest, the mass of the upper rigid body is combined with that of the lower rigid body and consequently, the rotational degree of freedom of the model vanishes. For that case, only three parameters are required for the model to take into account the influence of the backrest: the mass M_i transferred from upper to lower rigid body, the stiffness and the damping coefficients of the connection between the lower rigid body and the backrest. The general formulation of the model remains unchanged. Only the masses need to be modified through M_i, while the stiffness K_1 must be replaced by $K_1 + K_3$ and the damping coefficient C_1 by $C_1 + C_3$ to take into account the effect of the backrest Figs. 9 and 10.

Table 2 reports the parameter values applicable to 3 situations: (i) a flat rigid surface, (ii) a flat rigid surface covered with a foam of 20 thickness and (iii) an industrial seat equipped with a backrest.

Fig. 11 shows the comparison between calculated and measured apparent mass response for different back support conditions. The model predictions are in a good agreement with the apparent mass frequency response measured for the three postures:

(i) backrest off,
(ii) backrest on, contact in lumbar area,
(iii) backrest on, contact over the entire back.

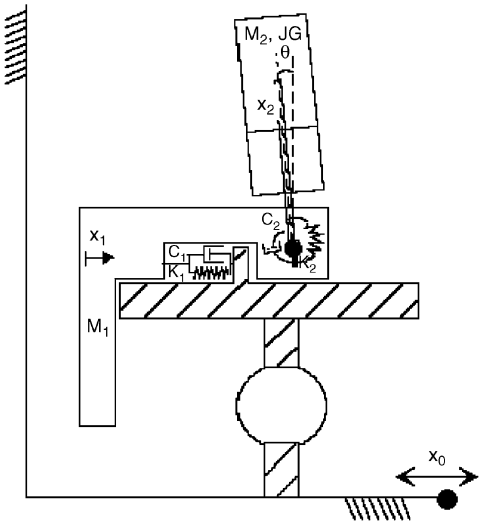

Fig. 9. A two rigid bodies model to describe the apparent mass of the seated subject exposed to fore-and-aft vibration (hands on lap, feet supported by the moving floor, backrest off).

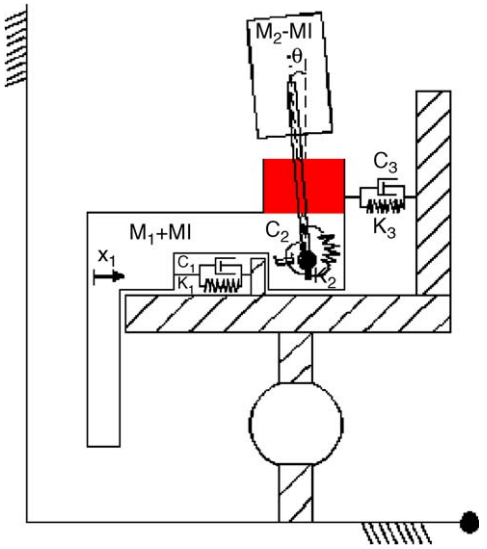

Fig. 10. Model extension to describe the effect of backrest.

4.4. The seat model

The seat model is limited to the suspension, which is represented by two pre-constrained steel springs, a damper, two end stop buffers and a slide system with friction. The design characteristics of these components were measured in the laboratory. The stiffness, damping and friction coefficients were evaluated by performing dynamic tests using a rigid mass of 70 kg mounted on the upper part of the suspension and applying sinusoidal vibration at the base. The spring stiffness was measured as being 5000 N/m, the damping coefficient of the damper as being 600 N/m/s and the friction coefficient in the slide system was measured as 0.07. The suspension stroke was established as being ± 13 mm and the end stop buffer static stiffness was measured as 38,000 N/m. The suspension model combines all these components with the parameter values as reported above.

4.5. The man/seat system model

The man/seat system model is built by combining the man and the seat models. The equations of motion of the man/seat system are derived as

$$M_0\ddot{x}_0 + K_1(x_0 - x_1) + C_1(\dot{x}_0 - \dot{x}_1) + K_s(x_0 - x_s) + C_s(\dot{x}_0 - \dot{x}_s) = 0, \tag{4}$$

$$M_1\ddot{x}_1 + K_1(x_1 - x_0) + C_1(\dot{x}_1 - \dot{x}_0) + M_2\ddot{x}_2 = 0, \tag{5}$$

$$J_G(\ddot{x}_1 - \ddot{x}_2) - \ddot{M}_2L^2\ddot{x}_2 + K_2(x_1 - x_2) + C_2(\dot{x}_1 - \dot{x}_2) = 0, \tag{6}$$

where M_0 is the seat mass mounted on the mobile part of the suspension, x_s, x_o the complex displacement at the seat pan and at the excitation point, respectively, K_s, C_s the stiffness and damping coefficients of the suspension.

The comparison between computed and measured apparent mass response for the case involving whole back support and unlocked suspension shows some discrepancies on the peak apparent mass and the frequency at which peak response occurs. The poor agreement is attributed to the fact that the model assumes a linear behaviour while the response of the subject is nonlinear.

Table 2
Model parameters applicable to 2 types of rigid seats and an industrial seat

		Flat rigid surface	Flat rigid surface covered with 20 mm	Industrial seat
Parameter values applicable to the base model	M_1 (kg)	31	31	31
	K_1 (N/m)	9585	9125	13605
	C_1 (N/m/s)	306	272	258
	M_2 (kg)	49	49	49
	K_2 (N m)	50	50	50
	C_2 (N m s)	32	28	37
	L (m)	0.4	0.4	0.4
Model extension to include the influence of the backrest	M_i (kg)			32
	K_3 (N/m)			14760
	C_3 (N/m/s)			340

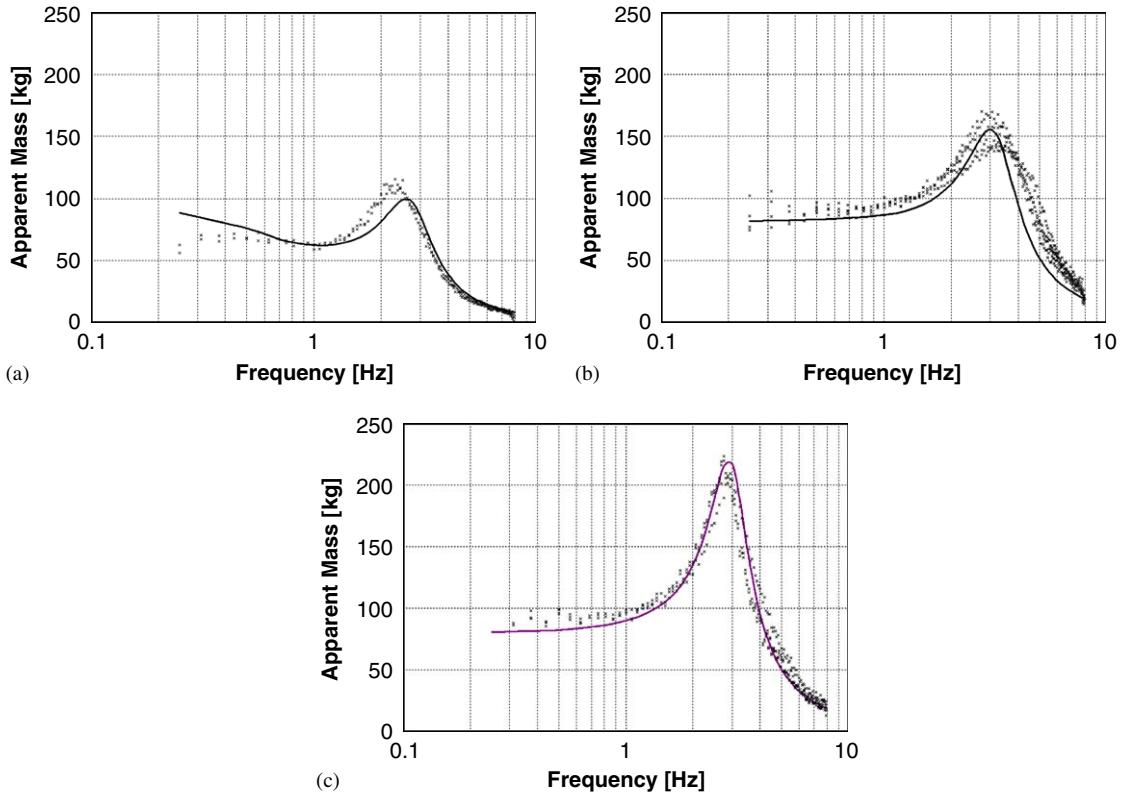

Fig. 11. Comparison between computed (—) and measured (^{xxxx}) apparent mass response for different back supports: (a) no backrest (b) backrest, lumbar support (c) backrest, whole back support.

5. A computational approach to design fore-and-aft suspensions

5.1. General mechanical specifications

In order to design technical solutions, guidelines are needed to define the required specifications. Design specifications for the fore-and-aft suspension are based on measurements and observations performed during field testing of wheel loader. The fore-and-aft suspension performance should be assessed by taking into

account three main mechanical features: the static strength of the suspension, the shock absorption capabilities and the vibration attenuation performance.

The static strength is described by the force which is slowly and progressively applied to the suspension to produce a relative displacement. While driving the vehicle, the forces exerted on the pedals and on the steering wheel are transferred to the seat. If the suspension response results in large relative displacements, the operator has difficulties to control his actions and feels uncomfortable. To overcome this effect, stiff springs can be used to limit relative displacements or the suspension stroke can be reduced.

The shock absorption capabilities are of importance mostly during operations involving bucket loading. Shocks are asymmetric and produce high relative displacements of the suspension only in the fore direction. Shock absorption has not been considered as part of the design concept in this work. Finally, vibration attenuation in the fore-and-aft direction is made necessary due to the pitching motion which results from vehicle riding on uneven tracks. Typical acceleration signals measured in that direction in wheel loaders show that the energy is mainly concentrated in a narrow frequency band centred around 1.6 Hz. Therefore, a method is applied to assess the suspension performance under stationary fore-and-aft vibration at a frequency of 1.6 Hz.

5.2. *Description of a numerical method to assess suspension performance under stationary fore-and-aft vibrations*

The response of the permanent model is computed using a sinusoidal excitation set at a frequency of 1.6 Hz. Four constraints are proposed to quantify the suspension performance. These are:

(1) The transmissibility between the lower body and the excitation point should be lower than 1. at the excitation frequency, i.e. the corresponding cut-off frequency is lower than the excitation frequency.
(2) The transmissibility between the upper body and the excitation point should be lower than 1. at the excitation frequency, i.e. the corresponding cut-off frequency is lower than the excitation frequency.
(3) The relative displacement of the suspension should be lower than the suspension stroke to ensure that no bottoming occurs.
(4) The interaction force calculated in the (K_3, C_3) connector should be lower than a preset value to limit the contact force between the driver's back and the backrest.

For each of the three postural conditions (no backrest, backrest with lumbar support, backrest with whole back support, see Fig. 11), the suspension features K_s and C_s which satisfy the four constraints defined previously are searched. Twelve inequations are therefore solved and their solutions (K_s, C_s) are reported in Fig. 12. The solution surface, for which (K_s, C_s) satisfy the 12 inequations, is delimited by 3 lines (see Fig. 12). Line (a) results from computation of constraint (1) associated with the model "without backrest", line (b) from computation of constraint (3) with the model "backrest with whole back support" and line (c) from computation of constraint (3) with the model "without backrest".

Preliminary calculations with a suspension stroke of ± 13 mm show that this condition is too restrictive. No suspension can be designed to fulfil this condition, therefore the suspension stroke is increased from ± 13 to ± 20 mm to obtain some solutions.

The maximal interaction force between the driver's back and the backrest is chosen to be equal to 100 N. With this value, the fourth constraint is not too restrictive. The original suspension with a stiffness of 10,000 N/m and a damping coefficient of 600 N/m/s does not satisfy the constraint on transmissibility between the lower body and the shaker associated to the model "without backrest". Decreasing the suspension stiffness from 10,000 to 3400 N/m allows a solution to be obtained which fulfils the 12 solved inequations.

In conclusion, the following characteristics are proposed for a new suspension design:

- the stroke may be increased from ± 13 to ± 20 mm,
- the spring stiffness may be reduced from 10,000 to 3400 N/m,
- the damping coefficient remains as is.

In order to estimate the performance of a seat with such design characteristics, numerical simulations were performed using the input signal recorded on the wheel loader during field tests as the excitation.

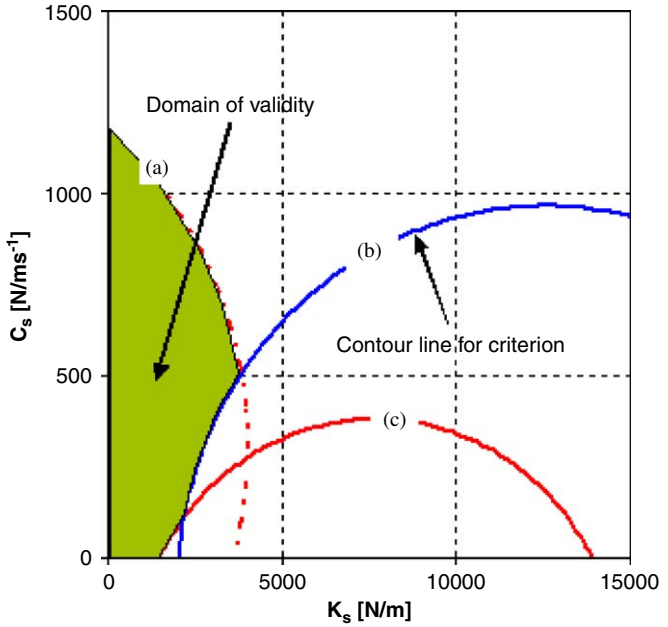

Fig. 12. K_s/C_s design diagram. Line (a) results from computation of constraint 1) associated with the model "without backrest", line (b) from computation of constraint 3) with the model "backrest with whole back support" and line (c) from computation of constraint 3) with the model "without backrest".

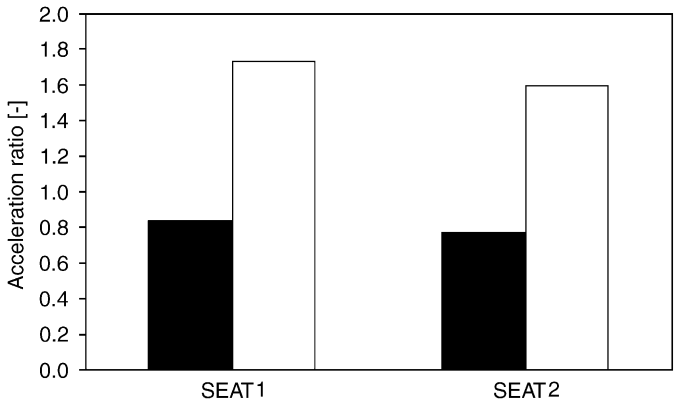

Fig. 13. Comparison of calculated seat factors $SEAT_1$ and $SEAT_2$ between the original (white column)and the new proposed suspension design (black column).

The performance of the seat suspension system was evaluated in terms of SEAT values calculated as the ratio of the frequency-weighted rms acceleration at the seat surface to that at the seat base and using the frequency weighting factors as specified in the ISO 2631 standard [1]:

$$\mathrm{SEAT}_1 = \frac{x_{\mathrm{wd1}}}{x_{\mathrm{wd}s}},$$

where x_{wd1} is the wd-frequency-weighted rms acceleration of the lower body, $x_{\mathrm{wd}s}$ the wd-frequency-weighted rms acceleration at the seat base:

$$\mathrm{SEAT}_2 = \frac{\sqrt{(1.4x_{\mathrm{wd1}})^2 + (0.8x_{\mathrm{wc2}})^2}}{\sqrt{(1.4x_{\mathrm{wd}s})^2 + (0.8x_{\mathrm{wc}s})^2}},$$

where x_{wc2} is the wc-frequency-weighted rms acceleration of the upper body, x_{wcs} the wc-frequency-weighted rms acceleration at the seat base.

Calculations were made for both the existing suspension and the optimized one. Results show (see Fig. 13) that the optimized suspension leads to a SEAT value which is approximately one half the value calculated for the existing suspension.

6. Conclusions

While driving off-road vehicles, drivers are exposed to whole-body vibration in all directions. Seat manufacturers supply products equipped with fore-and-aft suspension but only a few studies have reported on their performance. The aim of this work was to propose a computational approach that could be applied to design fore-and-aft suspensions for off-road vehicle seats. Measurements on a wheel loader were performed during normal operations in order to characterize the vibration and shocks transmitted at the seat attachment point. The cab was instrumented with cameras to observe the driver and his interactions with the vehicle. Performance of the fore-and-aft suspension was assessed by considering the static strength of the suspension and the vibration and shock attenuation. Wheel loader drivers are submitted to low frequency vibration resulting from regular motions on uneven surfaces. Suspensions should filter these vibration in order to reduce health disorders for the drivers. During certain specific tasks, such as filling the bucket, the operator is exposed to instantaneous shocks with high peak levels. The suspension system should absorb these shocks. In order to estimate the vibration attenuation performance of the suspension, a model of a sitting human body was developed and coupled to a seat model. The seat model was derived to represent the fore-and-aft suspension and the mass of the seat components located between the horizontal suspension and the driver. Two masses and three spring–damper connectors were used to model the dynamic behaviour of a sitting subject, the lower mass representing the lower limbs, the upper mass the upper limbs, the head and the trunk. Nine parameters were required to calculate the motions for both degrees of freedom. The apparent mass response of a seated human body was measured in the laboratory in the fore-and-aft direction. Several postures of the sitting subject were investigated. It was found that the initial contact surface between the back and the backrest could modify the measured apparent mass considerably. Model parameters were determined for three backrest conditions and comparisons were made between calculated and measured apparent masses for these conditions: no contact between back and backrest, contact in the lumbar area, contact all over the back surface. A preliminary study of the resulting model response was carried out under vibration set at a pre-defined frequency. Results were presented in a (K_s, C_s)-diagram, where K_s and C_s are the stiffness and the damping coefficient of the suspension, respectively. For each constraint that was applied, the diagram could define a region within which the constraints could be fulfilled. Constraints on the transmissibility between lower rigid body and excitation point, the transmissibility between the upper rigid body and the excitation point, the maximal interaction force between the back and the backrest and the maximal relative displacement of the suspension were investigated. A new set of design parameters was proposed for the suspension. The behaviour of the new suspension was simulated and the results compared with those of the existing one. These simulations used input signals recorded on the wheel loader during field tests and the resulting accelerations were post-treated and weighted according the ISO-2631 standard. Results showed the possibility of doubling the performance of the suspension to attenuate vibration.

7. Future work

The observations, the field measurements and the computational approach described above can be used to guide the design of horizontal suspensions to achieve a higher performance. The new proposed suspension needs to be validated by developing a prototype, whose behaviour may be checked in the laboratory. The prototype should verify design orientations which result from the model but on the other hand, it should consider also other points of technical specifications such as shock absorption and static strength. The ''best'' fore-and-aft suspension is surely the best compromise between vibration attenuation, shock absorption and static strength.

Acknowledgement

This investigation was partly supported by the European Commission under the 4th part of the Fifth Research and Technological Development Framework Programme (EU Contract no. GR3D-CT-2002-00827/ Vibseat consortium).

References

[1] International Organization for Standardization ISO 2631-1:1997(E), *Mechanical Vibration and Shock—Evaluation of Human Exposure to Whole-body Vibration*.
[2] P. Boisorieux, J.P. Galmiche, F. Maitre, Vibratory exposure of construction site plant drivers over a working day, presented at the *Third International Conference on Whole-Body Vibration*, Nancy, 2005.
[3] D. Roley, Reduction of vibrations on earth-moving machines, presented at the *Third International Conference on Whole-Body Vibration*, Nancy, 2005.
[4] International Organization for Standardization ISO 5008-2002: Tracteurs et matériels agricoles à roues—Mesurage des vibrations globales du corps du conducteur.
[5] G. Fleury, *Experimentelle Untersuchung der dynamischen Masse einer sitzenden Versuchsperson bei Schwingungen in der X-Richtung zur Bildung eines Modells*, Humanschwingungen, Darmstadt, VDI-Berichte 1821, 2004.
[6] T.E. Fairley, M.J. Griffin, The apparent mass of the seated human body in the fore-and-aft and lateral directions, *Journal of Sound and Vibration* 139 (2) (1990) 299–306.
[7] M. Plagenhoef, Anatomical data for analysing human motion, *Research Quarterly for Exercise and Sport* 54 (2) (1983) 169–178.